Amyloid precursor protein interacts with the mitochondrial phosphatase PGAM5 and regulates mitochondrial respiration

Kriti Shukla[1,2], Zhi Zhang[3], Kendra S. Plafker[1], Satoshi Matsuzaki[1], Casandra Salinas-Salinas[1], Yvonne Thomason[1], Samah Houmam[1,3,4], Dylan Barber[1,5], Anna Faakye[1,3], Kenneth M. Humphries[1,3], Scott M. Plafker[1], Jialing Lin[3], Heather C. Rice[1,2,3,4]

[1]Aging & Metabolism Research Program, Oklahoma Medical Research Foundation, Oklahoma City, OK, 73104, USA

[2]Department of Chemistry and Biochemistry, University of Oklahoma, Norman, OK, 73072, USA

[3]Department of Biochemistry & Physiology, University of Oklahoma Health Center, Oklahoma City, OK, 73104, USA

[4]Center for Geroscience and Healthy Brain Aging, University of Oklahoma Health Sciences Center, Oklahoma City, OK 73104

[5]Neuroscience Program, University of Oklahoma Health Center, Oklahoma City, OK, 73104, USA

Keywords

amyloid precursor protein (app)

phosphoglycerate mutase family member 5 (pgam5)

protein-protein interaction

brain metabolism

mitochondrial respiratory chain complex

Nuclear factor erythroid 2 p45-related factor 2 (Nrf2)

Alzheimer's disease

Abstract

Amyloid Precursor Protein (APP) has been reported to partially localize to mitochondria, and mitochondrial dysfunction is a key feature of Alzheimer's disease; however, the mechanisms linking APP to mitochondrial functions remain incompletely defined. In this study, we identified an interaction between APP and phosphoglycerate mutase family member 5 (PGAM5), a mitochondrial protein phosphatase. We confirmed their endogenous interaction in mouse brain

tissue and determined that APP and PGAM5 are both present at mitochondria-ER contact sites (MERCS) and. Using in vitro binding assays, we demonstrate a direct interaction between the linker region of APP and a region of PGAM5 that includes the Kelch-like ECH-associated protein 1 (Keap-1) binding domain. PGAM5 is known to anchor a portion of Nuclear factor erythroid 2 p45-related factor 2 (Nrf2) through Keap1 at the outer mitochondrial membrane and regulates mitochondrial respiration and stress responses. We found that the Nrf2-regulated genes Hmox1 (Heme oxygenase-1) and Nqo1 (NADH:quinone oxidoreductase 1), which are involved in mitochondrial respiration, are downregulated in APP KO astrocytes. Accordingly, mitochondria isolated from the brains of APP knockout (KO) mice have impaired substrate-specific respiration and electron transport chain (ETC) function. Together, these findings suggest that APP supports mitochondrial respiration by binding to PGAM5 and modulating Keap1-Nrf2 signaling.

Introduction

Mitochondrial dysfunction is a prominent feature of Alzheimer's disease (AD) and is thought to contribute to disease progression[1–4]. Multiple studies report increased oxidative stress[5,6], decreased ATP levels[7], and impaired brain metabolism in AD[8–10]. Amyloid Precursor Protein (APP) is the parent protein of Aβ peptides that aggregate to form plaques in Alzheimer's disease.[11,12] Although primarily localized to the secretory pathway, cell surface, and endocytic compartments, a portion of APP has been shown to be present at mitochondria and mitochondria-ER contact sites (MERCS)[13–16], which are also sites of APP processing[17,18]. Several studies have suggested a role of APP in mitochondrial functions[19–22]. Notably, APP alters mitochondrial mass[23], bioenergetics[20,24], mitophagy[25,26] and mitochondrial respiration[26,27]. The mechanisms by which APP affects mitochondrial function remain unclear, but understanding its protein-protein interactions at the mitochondria can help define its role[28].

Phosphoglycerate mutase family member 5 (PGAM5) emerged as a candidate interactor of the APP extracellular domain in an unbiased proteomics screen performed by Rice et al.[28]. PGAM5 is a mitochondrial phosphatase, with substrates that include B-cell lymphoma-extra large (Bcl-XL)[29], Dynamin-related protein 1 (DRP1)[30,31], FUN14 domain-containing protein 1 (FUNDC1)[32] and Mitofusin 2 (MFN2)[33], which are involved in mitochondrial mobility, mitophagy, redox homeostasis, respiration, or cell death.[29–32,34–36]. PGAM5 also regulates mitochondrial

respiration and stress response through the Keap1-Nrf2 pathway[36–41]. Under homeostatic conditions, Nrf2 is constitutively translated, ubiquitylated by Keap1/Cul3, and degraded by the proteasome[42,43]. In response to oxidative stress, modification of cysteines on Keap1 render it enzymatically inactive leading to a halt of the constitutive degradation of Nrf2. Nrf2 accumulates in the cytoplasm and then translocates to the nucleus, where it induces the transcription of antioxidant genes (e.g. *Hmox1 and Nqo1*) to restore redox homeostasis and support mitochondrial respiration[36,42,43]. A subset of Nrf2 is tethered to the outer mitochondrial membrane through a ternary complex with PGAM5 and Keap1. Knockdown of PGAM5 or Keap1 activates Nrf2 target gene expression [36,40] . The PGAM5-Keap1-Nrf2 complex has been implicated in both stress-induced mitochondrial retrograde trafficking[37] and mitochondrial respiration[36] .

In this study, we establish an interaction between APP and PGAM5 that is mediated by a region of PGAM5 that includes the Keap1-binding domain. Consistent with disrupted PGAM5-Keap1-Nrf2 signaling, expression of the Nrf2 target genes *Hmox1 and Nqo1* are reduced in APP KO astrocytes. We show that mitochondria from APP KO mouse brains have impaired substrate-specific respiration and electron transport chain (ETC) function. Together, these findings suggest a role for APP in regulating mitochondrial respiration by binding to PGAM5 and regulating Keap1-Nrf2 signaling pathway.

Results

APP and PGAM5 interact endogenously and are both present at mitochondria-ER contact sites

To investigate a potential mechanism underlying APP function in mitochondria, we followed up on a prior proteomics screen performed by Rice et. al. [28] identifying the mitochondrial phosphatase PGAM5 as a candidate interactor of the APP ectodomain[4]. To determine whether APP and PGAM5 interact endogenously, PGAM5 was immunoprecipitated (IPed) from brain extracts of wild-type (WT) mice or PGAM5 knockout (KO) mice, as a negative control. APP co-IPed with PGAM5 in WT but was not detected in IPs from PGAM5 KO extracts, indicating that APP and PGAM5 interact endogenously in mouse brain (Figure 1A). To confirm that a portion of APP and PGAM5 localize to common subcellular compartments, we performed subcellular fractionation of WT mouse brains to isolate mitochondria, ER, and mitochondria-ER contact

sites (MERCS). Both young (3mo) and old (12mo) mice showed similar subcellular distribution of APP and PGAM5, so both ages were plotted together. Consistent with the literature, APP was found to localize at the ER but interestingly, a significant amount was also present at MERCS (Figure 1B,C). On the other hand, PGAM5 was also found to be present at MERCS while predominantly being present at the mitochondria (Figure 1B,D). This data showed that both APP and PGAM5 can be found at MERCS (Figure 1B-D), suggesting MERCS as a potential site for their interaction.

APP interacts with a region of PGAM5 containing the Keap1 binding domain

Next, we used *in vitro* binding assays to determine whether APP and PGAM5 can directly interact and to narrow the binding regions responsible for this interaction. Since both APP and PGAM5 full-length proteins have transmembrane domains (TM), we used the recombinant soluble APP (sAPPα, aa1-496) (Figure 2A) and truncated PGAM5 constructs (Figure 2B). Amino acids 1-54 (TM domain) of PGAM5 were removed to make PGAM5Δ54 while PGAM5Δ90 had additional 36 amino acids (containing the multimerization motif;MM and Keap1-binding domain;KBD) removed[4734,36,48]. We used Protein G Sepharose beads to pull down Fc-tagged sAPPα incubated with either PGAM5Δ54 or PGAM5Δ90. PGAM5Δ54 but not PGAM5Δ90 was pulled-down with sAPPα-Fc, indicating that the interaction requires the N-terminal region of PGAM5 containing the KBD and MM (Figure 2C). Isothermal titration calorimetry (ITC) with sAPPα (without an Fc tag) and PGAM5Δ54, revealed a dissociation constant (K_d) of 3.45 µM and a binding stoichiometry of N = 0.114 (Figure 2D). Then, to narrow down the domain in APP required for binding to PGAM5, we used Protein G Sepharose beads to pull down individual Fc-tagged domains of APP (Growth factor-like domain;GFLD-Fc, Copper binding domain;CuBD-Fc, Extension domain;ExD-Fc, Acidic domain;AcD-Fc and Extracellular 2;E2-Fc) incubated with PGAM5Δ54. PGAM5Δ54 was most efficiently pulled-down with ExD-Fc followed by AcD-Fc (Figure 2E-F). Together, these results suggest that the linker region of APP (constituted by AcD and ExD) and the N-terminal amino acids (aa55-89) of PGAM5 (containing Keap1 binding domain) are critical for binding between these two proteins.

Transcription of Nrf2-regulated genes is altered in APP KO astrocytes

To understand the functional implications of binding of APP to the N-terminal region of PGAM5 containing the Keap-1 binding domain, we investigated whether the Keap1-Nrf2 pathway is

affected by the presence of APP. We examined Nrf2-dependent gene expression in primary astrocytes isolated from the brains of WT or APP KO mice. Astrocytes were chosen based on prior literature demonstrating a critical role for APP in mitochondrial function in astrocytes[44]. Total RNA was isolated from WT or APP KO astrocytes and transcript levels of established Nrf2 target genes (*Hmox1, Nqo1, Gclc, Gclm, and Txnrd1*) were quantified by qPCR. Both *Hmox1* and *Nqo1* transcripts were significantly reduced in APP KO astrocytes compared to WT controls. No significant differences were observed for *Gclc*, *Gclm*, or *Txnrd1* (Figure 3).

Mitochondria isolated from APP KO mouse brains have impaired respiration

Since the basal expression of *Nqo1* and *Hmox1* was decreased in APP KO conditions and both these genes are essential for maintaining redox homeostasis that permit efficient NADH oxidation at Complex I[45,46], we investigated if loss of APP also affects mitochondrial respiration and ETC. We performed respiratory measurements in freshly isolated mitochondria from WT vs APP KO mouse brains. APP KO mitochondria showed significantly decreased pyruvate (Figure 4A) and glutamate-mediated (Figure 4B) respiration with no changes observed in succinate-mediated respiration (Figure 4C) as compared to WT, indicating an impairment in maximal NADH-linked mitochondrial respiration whereas Complex II–dependent respiration (succinate) remains intact. Additionally, we measured the effect of APP KO on Complex I activity, the rate limiting step of the ETC and NADH oxidase activity as a measure of total ETC activity. Our findings showed a significant decrease in NADH oxidase activity in APP KO mitochondria (Figure 4D) and a decreasing but non-statistically significant trend in complex I activity (Figure 4E). Taken together, these findings highlight a crucial physiological role of APP in maintaining Complex I function and NADH-linked respiration in brain mitochondria.

Discussion

In this study, we identify the mitochondrial protein phosphatase PGAM5 as an interactor of APP. Both APP and PGAM5 were found to interact endogenously and both were present at MERCS. Interestingly, the amount of APP present at MERCS was comparable to the amount at ER, suggesting a crucial role of APP at these inter-organelle sites. Previous studies have identified MERCS as an APP processing site [17,18], and our findings suggest a functional role for APP localized to MERCS[23,24]. Our ITC data showed binding between APP and PGAM5 with a

binding stoichiometry (N) of 0.114, which is consistent with a dodecameric PGAM5 complex associated with an APP dimer. APP is known to form homodimers through its E1 and transmembrane domains, which has been implicated in its processing and function[47]. PGAM5, on the other hand, assembles into higher-order oligomers, predominantly forming dodecamers as well as dimers, that are critical for its functions[30,32,48]. The APP-PGAM5 interaction requires a region of PGAM5 containing the Keap1-binding domain, suggesting that APP may compete with Keap1 for its binding to PGAM5. PGAM5 is known to tether Nrf2 at the outer mitochondrial membrane through Keap1 and regulates the amount of Nrf2 translocating into the nucleus for gene expression[40]. Consistent with this, we find that transcription of Nrf2 target genes, *Nqo1* and *Hmox1,* is significantly reduced in APP KO primary astrocytes under physiological conditions. Both NQO1 and HMOX1 are critical components of the Nrf2 antioxidant network that preserve mitochondrial redox homeostasis and regulate respiration[49–51]. NQO1 limits quinone redox cycling and supports respiration by maintaining NAD^+/NADH balance[52,53], while HMOX1 helps mitigate oxidative stress and supports ETC[54,55]. Taken together, these findings suggest that the APP-PGAM5 interaction at MERCS may regulate mitochondrial respiration and stress response through modulation of Keap1-Nrf2 signaling.

We further show that APP deficiency leads to a selective reduction in glutamate- and pyruvate-driven respiration. This substrate-specific defect points to a dysfunction upstream of or at Complex I, rather than a global failure of the electron transport chain or mitochondrial integrity. Consistent with this interpretation, we observe a reduction in NADH oxidase activity and a downward trend in Complex I enzymatic activity in APP KO mitochondria. Together, these results position APP as a regulator of NADH-linked respiration in the brain and suggest that impaired NADH-dependent respiration may not only limit electron transport capacity but also promote oxidative imbalance and bioenergetic insufficiency. In this context, diminished Complex I function could enhance electron leak and reactive oxygen species generation while simultaneously constraining ATP synthesis. When considered alongside previous evidence that manipulation of APP alters ETC activity, ATP levels, and mitochondrial biogenesis[26,56], our findings strengthen the conclusion that APP is an essential contributor to mitochondrial bioenergetics.

Based on our findings, we propose a model in which APP helps maintain Nrf2-dependant gene regulation by competing with Keap1 to bind to PGAM5 at MERCS. In WT conditions, APP binding to PGAM5 may promote displacement of Keap1-bound Nrf2, enabling Nrf2 accumulation at the cytoplasm and eventual nuclear translocation that in turn leads to gene expression (Figure 5A). On the other hand, in the absence of APP, Keap1-bound Nrf2 is constantly tethered to PGAM5 and is unable to translocate to the nucleus to turn on the gene transcription and hence the expression of genes required to maintain mitochondrial respiration and redox balance is reduced (Figure 5B). This model provides a mechanistic basis for mitochondrial bioenergetic deficits often observed upon APP loss[61–63] and warrants future studies to determine whether mitochondrial dysfunction observed in AD arises from loss of normal APP function.

Experimental procedures

(see Supporting information for details)

Mouse models

All experiments were conducted following a protocol approved by the Oklahoma Medical Research Foundation's (OMRF) Institutional Animal Care and Use Committee prior to any animal work.

Co-immunoprecipitation, Western blotting, Protein pull-down assays

see Supporting information for details

Subcellular fractionation

Mouse brain mitochondria and mitochondria-ER contact sites (MERCS) were isolated as previously described [57].

Plasmids

APP plasmids were provided by Dr. Bart De Strooper and Dr. Joris de Wit (VIB-KU Leuven, Belgium)[28]. PGAM5 plasmids were provided by Dr. Apirat Chaikuad (Institute for Pharmaceutical Chemistry, Johann Wolfgang Goethe-University and Buchmann Institute for Molecular Life Sciences, Germany)[48].

Purification of recombinant soluble APP proteins

APP fragments with a C-terminal Fc tag were expressed by transfection in HEK293T cells and purified using Protein-G Sepharose 4 Fast Flow resin.

Purification of recombinant soluble PGAM5 proteins

PGAM5 plasmids were expressed in BL21 Rosetta competent *E. coli* cells using 0.5mM IPTG. The proteins were purified using Nickel(II)-NTA agarose beads.

Isothermal Titration Calorimetry

All ITC experiments were performed on a MicroCal PEAQ-ITC system at OU Protein Production and Characterization Core. The raw ITC data were fitted to a single binding site model using the MicroCal PEAQ-ITC analysis software provided by the manufacturer.

Primary Mouse Astrocyte Culture

Primary astrocytes were isolated from whole brains of postnatal day 0–5 (P0–P5) C57BL/6J or APP KO mice using a differential adhesion–based protocol[58].

qPCR

Total RNA extracted from primary mouse astrocytes was used to synthesize cDNA. Real-time quantitative PCR was performed using PowerUp™ SYBR® Green PCR Master Mix (Applied Biosystems) and the primers for the genes- *Hmox1, Nqo1, Gclc, Gclm*, *Txnrd1* and *Actb.* The mRNA levels of target genes were normalized to *ActB* by untreated WT sample values.

Respiratory measurements with isolated mitochondria

Mouse brain mitochondria were isolated and mitochondrial respiration measurements were performed according to established protocols.[57,59]

ETC enzyme activity assays

NADH oxidase activity was measured as previously described.[60]

Data Availability

All data described in the manuscript are contained within the manuscript.

Supporting Information

This article contains supporting information[28,48,57–61]

Conflict of Interest

The authors declare that they have no conflicts of interest with the contents of this article.

Acknowledgements

This work was supported by the National Institutes of Health (R35GM142726, P20GM125528 to H.C.R.), Institutional Development Award (IDeA) from the National Institute of General Medical Sciences (NIGMS) of the National Institutes of Health (NIH) (P20GM103640 to J.L. as a junior investigator), and the Presbyterian Health Foundation (Pilot Research Funding to H.C.R.; Bridge Funding to J.L..). APP plasmids were provided by Dr. Bart De Strooper and Dr. Joris de Wit (VIB-KU Leuven, Belgium)[28]. PGAM5 plasmids were provided by Dr. Apirat Chaikuad (Institute for Pharmaceutical Chemistry, Johann Wolfgang Goethe-University and Buchmann Institute for Molecular Life Sciences, Germany)[48]. The ITC experiments were done at OU Protein Production and Characterization Core facility, supported by IDeA from the NIGMS of NIH (P20GM103640 and P30GM145423), the OU Vice President for Research and Partnerships, and the OU College of Arts and Sciences. PGAM5 KO mouse strain was provided by Dr. Yishi Jin with permission from Dr. Michael Lenardo who originally developed the mice[61]. Data analysis was supported by the OMRF Center for Biomedical Data Sciences. Figure 5 schematic was created in Biorender-https://BioRender.com/ftsycbt

Bibliography

1. Serrano-Pozo, A., Frosch, M. P., Masliah, E. & Hyman, B. T. Neuropathological alterations in Alzheimer disease. *Cold Spring Harb. Perspect. Med.* **1**, (2011).

2. Misrani, A., Tabassum, S. & Yang, L. Mitochondrial Dysfunction and Oxidative Stress in Alzheimer's Disease. *Frontiers in Aging Neuroscience* vol. 13 Preprint at https://doi.org/10.3389/fnagi.2021.617588 (2021).

3. Ashleigh, T., Swerdlow, R. H. & Beal, M. F. The role of mitochondrial dysfunction in Alzheimer's disease pathogenesis. *Alzheimer's and Dementia* **19**, 333–342 (2023).

4. Pszczołowska, M. *et al.* Mitochondrial disorders leading to Alzheimer's disease—perspectives of diagnosis and treatment. *GeroScience* vol. 46 2977–2988 Preprint at https://doi.org/10.1007/s11357-024-01118-y (2024).

5. Dumont, M. *et al.* Reduction of oxidative stress, amyloid deposition, and memory deficit by manganese superoxide dismutase overexpression in a transgenic mouse model of Alzheimer's disease. *The FASEB Journal* **23**, 2459 (2009).

6. Wang, J., Xiong, S., Xie, C., Markesbery, W. R. & Lovell, M. A. Increased oxidative damage in nuclear and mitochondrial DNA in Alzheimer's disease. *J. Neurochem.* **93**, 953–962 (2005).

7. Zhang, C., Rissman, R. A. & Feng, J. Characterization of ATP Alternations in an Alzheimer's Transgenic Mouse Model. *J. Alzheimers Dis.* **44**, 375 (2015).

8. Gasparini, L. *et al.* Energy metabolism inhibition impairs amyloid precursor protein secretion from Alzheimer's fibroblasts. *Neurosci. Lett.* **263**, 197–200 (1999).

9. Li, P. A., Hou, X. & Hao, S. Mitochondrial biogenesis in neurodegeneration. *J. Neurosci. Res.* **95**, 2025–2029 (2017).

10. Singulani, M. P. *et al.* Impairment of PGC-1α-mediated mitochondrial biogenesis precedes mitochondrial dysfunction and Alzheimer's pathology in the 3xTg mouse model of Alzheimer's disease. *Exp. Gerontol.* **133**, (2020).

11. Glenner, G. G. & Wong, C. W. Alzheimer's disease: Initial report of the purification and characterization of a novel cerebrovascular amyloid protein. *Biochem. Biophys. Res. Commun.* **120**, 885–890 (1984).

12. Masters, C. L. *et al.* Amyloid plaque core protein in Alzheimer disease and Down syndrome. *Proc. Natl. Acad. Sci. U. S. A.* **82**, 4245 (1985).

13. Devi, L., Prabhu, B. M., Galati, D. F., Avadhani, N. G. & Anandatheerthavarada, H. K. Accumulation of Amyloid Precursor Protein in the Mitochondrial Import Channels of Human Alzheimer's Disease Brain Is Associated with Mitochondrial Dysfunction. *The Journal of Neuroscience* **26**, 9057 (2006).

14. Anandatheerthavarada, H. K., Biswas, G., Robin, M. A. & Avadhani, N. G. Mitochondrial targeting and a novel transmembrane arrest of Alzheimer's amyloid precursor protein impairs mitochondrial function in neuronal cells. *Journal of Cell Biology* **161**, 41–54 (2003).

15. Area-Gomez, E. *et al.* Upregulated function of mitochondria-associated ER membranes in Alzheimer disease. *EMBO J.* **31**, 4106–4123 (2012).

16. Bhattacharyya, R. *et al.* Axonal generation of amyloid-β from palmitoylated APP in mitochondria-associated endoplasmic reticulum membranes. *Cell Rep.* **35**, (2021).

17. Del Prete, D. *et al.* Localization and Processing of the Amyloid-β Protein Precursor in Mitochondria-Associated Membranes. *Journal of Alzheimer's Disease* **55**, 1549 (2017).

18. Schreiner, B., Hedskog, L., Wiehager, B. & Ankarcrona, M. Amyloid-β Peptides are Generated in Mitochondria-Associated Endoplasmic Reticulum Membranes. *Journal of Alzheimer's Disease* **43**, 369–374 (2015).

19. Gabuzda, D., Busciglio, J., Chen, L. B., Matsudaira, P. & Yankner, B. A. Inhibition of energy metabolism alters the processing of amyloid precursor protein and induces a potentially amyloidogenic derivative. *Journal of Biological Chemistry* **269**, 13623–13628 (1994).

20. Wilkins, H. M. & Swerdlow, R. H. Amyloid precursor protein processing and bioenergetics. *Brain Res. Bull.* **133**, 71–79 (2017).

21. Strope, T. A. & Wilkins, H. M. Amyloid Precursor Protein and Mitochondria. *Curr. Opin. Neurobiol.* **78**, 102651 (2023).

22. Strope, T. A. & Wilkins, H. M. The reciprocal relationship between amyloid precursor protein and mitochondrial function. *J. Neurochem.* **168**, 2275–2284 (2024).

23. An, Y. A. *et al.* Dysregulation of Amyloid Precursor Protein Impairs Adipose Tissue Mitochondrial Function and Promotes Obesity. *Nat. Metab.* **1**, 1243 (2019).

24. Ferrer, I. Altered mitochondria, energy metabolism, voltage-dependent anion channel, and lipid rafts converge to exhaust neurons in Alzheimer's disease. *J. Bioenerg. Biomembr.* **41**, 425–431 (2009).

25. Wilkins, H. M. Mitochondrial Localized Amyloid Precursor Protein Alters Mitochondrial Function and Mitophagy. *Alzheimer's & Dementia* **19**, e074226 (2023).

26. Strope, T. A. *et al.* Amyloid-β protein precursor modulates mitophagy and mitochondrial function through its cellular localization. *J. Alzheimers Dis.* **107**, 277 (2025).

27. Lopez Sanchez, M. I. G. *et al.* Amyloid precursor protein drives down-regulation of mitochondrial oxidative phosphorylation independent of amyloid beta. *Sci. Rep.* **7**, (2017).

28. Rice, H. C. *et al.* Secreted Amyloid-β Precursor Protein Functions as a GABABR1a Ligand to Modulate Synaptic Transmission. *Science* **363**, (2019).

29. Lo, S. C. & Hannink, M. PGAM5, a Bcl-XL-interacting Protein, Is a Novel Substrate for the Redox-regulated Keap1-dependent Ubiquitin Ligase Complex. *Journal of Biological Chemistry* **281**, 37893–37903 (2006).

30. Nag, S., Szederkenyi, K., Yip, C. M. & McQuibban, G. A. PGAM5 cleavage and oligomerization equilibrates mitochondrial dynamics under stress by regulating DRP1 function. *J. Cell Sci.* **138**, jcs263903 (2025).

31. Yu, B. *et al.* Mitochondrial phosphatase PGAM5 modulates cellular senescence by regulating mitochondrial dynamics. *Nature Communications 2020 11:1* **11**, 1–17 (2020).

32. Ma, K. *et al.* Dynamic PGAM5 multimers dephosphorylate BCL-xL or FUNDC1 to regulate mitochondrial and cellular fate. *Cell Death & Differentiation 2019 27:3* **27**, 1036–1051 (2019).

33. Nag, S. *et al.* PGAM5 is an MFN2 phosphatase that plays an essential role in the regulation of mitochondrial dynamics. *Cell Rep.* **42**, 112895 (2023).

34. Lu, W. *et al.* Mitochondrial Protein PGAM5 Regulates Mitophagic Protection against Cell Necroptosis. *PLoS One* **11**, e0147792 (2016).

35. Wang, Z., Jiang, H., Chen, S., Du, F. & Wang, X. The Mitochondrial Phosphatase PGAM5 Functions at the Convergence Point of Multiple Necrotic Death Pathways. *Cell* **148**, 228–243 (2012).

36. Safakli, R. N., Gray, S., Bernardi, N. & Smyrnias, I. Unveiling a novel signalling pathway involving NRF2 and PGAM5 in regulating the mitochondrial unfolded protein response in stressed cardiomyocytes. *Int. J. Biochem. Cell Biol.* **178**, 106704 (2025).

37. O'Mealey, G. B. *et al.* A PGAM5-KEAP1-Nrf2 complex is required for stress-induced mitochondrial retrograde trafficking. *J. Cell Sci.* **130**, 3467–3480 (2017).

38. Baird, L. & Yamamoto, M. The Molecular Mechanisms Regulating the KEAP1-NRF2 Pathway. *Mol. Cell. Biol.* **40**, e00099-20 (2020).

39. Tong, K. I. *et al.* Keap1 Recruits Neh2 through Binding to ETGE and DLG Motifs: Characterization of the Two-Site Molecular Recognition Model. *Mol. Cell. Biol.* **26**, 2887 (2006).

40. Lo, S. C. & Hannink, M. PGAM5 tethers a ternary complex containing Keap1 and Nrf2 to mitochondria. *Exp. Cell Res.* **314**, 1789–1803 (2008).

41. Ma, S. *et al.* Targeting mitochondrial phosphatase PGAM5 alleviates ferroptosis and acute pancreatitis by upregulating NRF2-mediated FSP1 expression. *Cell Death Dis.* **17**, 252 (2026).

42. Zeb, A. *et al.* A novel role of KEAP1/PGAM5 complex: ROS sensor for inducing mitophagy. *Redox Biol.* **48**, 102186 (2021).

43. Baird, L. & Yamamoto, M. The Molecular Mechanisms Regulating the KEAP1-NRF2 Pathway. *Mol. Cell. Biol.* **40**, e00099-20 (2020).

44. Montagna, E. *et al.* In vivo Ca2+ imaging of astrocytic microdomains reveals a critical role of the amyloid precursor protein for mitochondria. *Glia* **67**, 985–998 (2019).

45. Chiang, S. K., Chen, S. E. & Chang, L. C. The Role of HO-1 and Its Crosstalk with Oxidative Stress in Cancer Cell Survival. *Cells* **10**, 2401 (2021).

46. Lee, W. S., Ham, W. & Kim, J. Roles of NAD(P)H:quinone Oxidoreductase 1 in Diverse Diseases. . **11**, 1301 (2021).

47. Scheuermann, S. *et al.* Homodimerization of Amyloid Precursor Protein and Its Implication in the Amyloidogenic Pathway of Alzheimer's Disease. *Journal of Biological Chemistry* **276**, 33923–33929 (2001).

48. Chaikuad, A. *et al.* Structures of PGAM5 Provide Insight into Active Site Plasticity and Multimeric Assembly. *Structure(London, England:1993)* **25**, 1089 (2017).

49. Loboda, A., Damulewicz, M., Pyza, E., Jozkowicz, A. & Dulak, J. Role of Nrf2/HO-1 system in development, oxidative stress response and diseases: an evolutionarily conserved mechanism. *Cell. Mol. Life Sci.* **73**, 3221 (2016).

50. Jaber, S. M. *et al.* Idebenone Has Distinct Effects on Mitochondrial Respiration in Cortical Astrocytes Compared to Cortical Neurons Due to Differential NQO1 Activity. *The Journal of Neuroscience* **40**, 4609 (2020).

51. Haefeli, R. H. *et al.* NQO1-Dependent Redox Cycling of Idebenone: Effects on Cellular Redox Potential and Energy Levels. *PLoS One* **6**, e17963 (2011).

52. Gray, J. P., Karandrea, S., Burgos, D. Z., Jaiswal, A. A. & Heart, E. A. NAD(P)H-dependent Quinone Oxidoreductase 1 (NQO1) and Cytochrome P450 Oxidoreductase (CYP450OR) differentially regulate menadione-mediated alterations in redox status, survival and metabolism in pancreatic β-cells. *Toxicol. Lett.* **262**, 1 (2016).

53. Dinkova-Kostova, A. T. & Talalay, P. NAD(P)H:quinone acceptor oxidoreductase 1 (NQO1), a multifunctional antioxidant enzyme and exceptionally versatile cytoprotector. *Arch. Biochem. Biophys.* **501**, 116–123 (2010).

54. Chiang, S. K., Chen, S. E. & Chang, L. C. The Role of HO-1 and Its Crosstalk with Oxidative Stress in Cancer Cell Survival. *Cells* **10**, 2401 (2021).

55. Carr, J. F. *et al.* Heme Oxygenase-1 Supports Mitochondrial Energy Production and Electron Transport Chain Activity in Cultured Lung Epithelial Cells. *Int. J. Mol. Sci.* **21**, 6941 (2020).

56. Wang, Y. *et al.* Lost region in amyloid precursor protein (APP) through TALEN-mediated genome editing alters mitochondrial morphology. *Sci. Rep.* **6**, (2016).

57. Wieckowski, M. R. M. R., Giorgi, C., Lebiedzinska, M., Duszynski, J. & Pinton, P. Isolation of mitochondria-associated membranes and mitochondria from animal tissues and cells. *Nat. Protoc.* **4**, 1582–1590 (2009).

58. Güler, B. E., Krzysko, J. & Wolfrum, U. Isolation and culturing of primary mouse astrocytes for the analysis of focal adhesion dynamics. *STAR Protoc.* **2**, 100954 (2021).

59. Li, P. *et al.* The loss of cardiac SIRT3 decreases metabolic flexibility and proteostasis in an age-dependent manner. *GeroScience 2022 45:2* **45**, 983–999 (2022).

60. Mendez Garcia, M. F. *et al.* Increased cardiac PFK-2 protects against high-fat diet-induced cardiomyopathy and mediates beneficial systemic metabolic effects. *iScience* **26**, 107131 (2023).

61. Lu, W. *et al.* Genetic deficiency of the mitochondrial protein PGAM5 causes a Parkinson's-like movement disorder. *Nat. Commun.* **5**, (2014).

Figure legends

Figure 1. APP and PGAM5 interact endogenously and are both present at mitochondria-ER contact sites (A). Western blot showing immunoprecipitated PGAM5 and co-immunoprecipitated APP in WT and PGAM5 KO (4mo, males) mouse brains. **(B).** Western blot showing subcellular localization of PGAM5 and APP in WT (C57Bl6, 3-12 months old, females) mouse brains. The cellular compartments shown are Whole brain, Crude mitochondria,

Mitochondria, Mitochondria-ER contact sites (MERCS) and Endoplasmic reticulum (ER). The purity of each sample was validated by its marker protein (TOM20 (Translocase of Outer Mitochondrial Membrane 20), Mitochondria; ATPase (Adenosine Triphosphatase), MERCS; BiP (Binding Immunoglobulin Protein), ER). **(C-D).** Graphs showing western blot quantification indicating levels of C. APP protein and D. PGAM5 protein. Values shown are band intensity means ± SD (*n* =7). One-way ANOVA tests were performed for each graph, *** ($P < 0.01$), **** ($P < 0.001$), ns (non-significant).

Figure 2. APP interacts with a region of PGAM5 containing the Keap1 binding domain (A-B). Schematics showing domains (GFLD; Growth-like factor domain, CuBD; Copper-binding domain, AcD; Acidic domain, ExD; Extension domain, E2, JMR; Juxtamembrane Region, TM; Transmembrane, AICD; APP intracellular domain, MM; Multimerization motif, KBD; Keap1 binding domain, PGAM; Phosphoglycerate mutase) and recombinant protein constructs (sAPPα, PGAM5-Δ90 and PGAM5-Δ54) of APP (pink) and PGAM5 (yellow). **B.** Coomassie stained SDS-PAGE gels of bound and unbound material from Fc-pulldowns of sAPP-Fc with PGAM5Δ54 or PGAM5Δ90 purified proteins, **C.** Binding curve from ITC done using the sAPPα and PGAM5-Δ54 purified proteins (n=3). **(D-E).** D. Coomassie stained SDS-PAGE gels of bound and unbound material from Fc-pulldowns of sAPP-Fc, GFLD-Fc, CuBD-Fc, ExD-Fc, AcD-Fc, E2-Fc and beads with PGAM5Δ54 purified protein and E. Quantification of pull-down assays showing net PGAM5Δ54 bound and pulled down with each Fc-tagged sAPPα domain. Values shown are means ± SD (*n* =5 - 6) and the statistics were performed using Dunnett's multiple comparison test. ***** ($P < 0.0001$).

Figure 3. APP affects Nrf2-regulated gene expression. Plot showing relative mRNA expression of Nrf2-regulated genes in cultured primary astrocytes isolated from WT and APP KO mouse brains, measured by RT-qPCR. Values shown are the means ± SD (*n* = 8-9) and the statistics were performed using two-way ANOVA, followed by Tukey's multiple comparison test. ***** ($P < 0.0001$), ns (non-significant).

Figure 4. Isolated mitochondria from APP KO mice brain have impaired respiration. (A-C). Graphs showing maximum respiration by utilizing different oxidizable substrates (A. Pyruvate/malate, B. glutamate/malate, C. Succinate), in the mitochondria isolated from 6-8 months old APP KO mouse brains. Values shown are the means ± SD (*n* =4 - 6). Two-tailed

paired t-tests were performed for each graph. **(D-E).** Graphs showing impaired ETC in APP KO mitochondria as indicated by D. decreased Complex I activity and E. NADH oxidase activity. Values shown are means ± SD (*n* =5 - 6). Two-tailed paired t-test was performed for each graph, * ($P < 0.05$), ns (non-significant).

Figure 5. Proposed model by which APP affects mitochondrial respiration. A. In WT cells, APP localized to MERCS can bind to PGAM5 and displace Keap1. This releases Keap1-bound Nrf2 to the cytoplasm where Nrf2 dissociates from Keap1, accumulates, and subsequently translocates to the nucleus to activate transcription of genes that maintain normal mitochondrial respiration. **B.** In APP KO cells, Nrf2 remains bound to PGAM5 at the mitochondria, leading to reduced Nrf2 translocation to the nucleus and reduced transcription of its target genes. This reduced Nrf2 signaling in the absence of APP leads to impaired mitochondrial respiration. The schematic was created in BioRender. Rice, H. (2026) https://BioRender.com/ftsycbt.

Figure 1

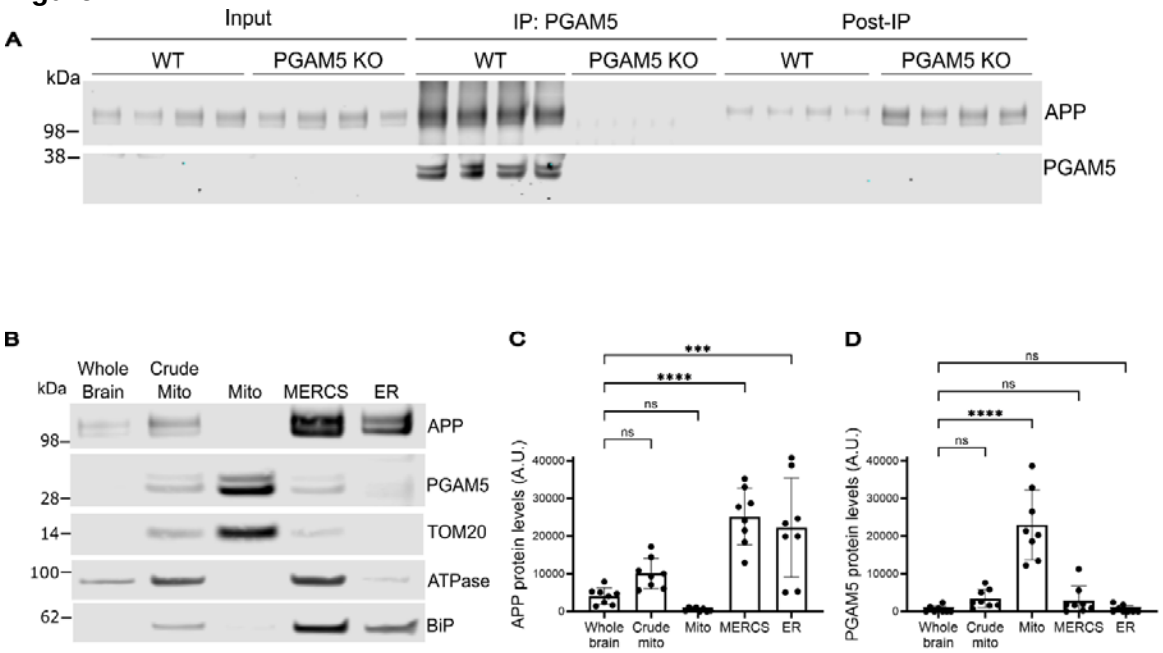
A
Input
IP: PGAM5
Post-IP
WT
PGAM5 KO
WT
PGAM5 KO
WT
PGAM5 KO
kDa
98–
38–
APP
PGAM5
B
Whole Brain
Crude Mito
Mito
MERCS
ER
kDa
98–
28–
14–
100–
62–
APP
PGAM5
TOM20
ATPase
BiP
C
APP protein levels (A.U.)
40000
30000
20000
10000
0
***
****
ns
ns
Whole brain
Crude mito
Mito
MERCS
ER
D
PGAM5 protein levels (A.U.)
40000
30000
20000
10000
0
ns
ns
****
ns
Whole brain
Crude mito
Mito
MERCS
ER

Figure 2

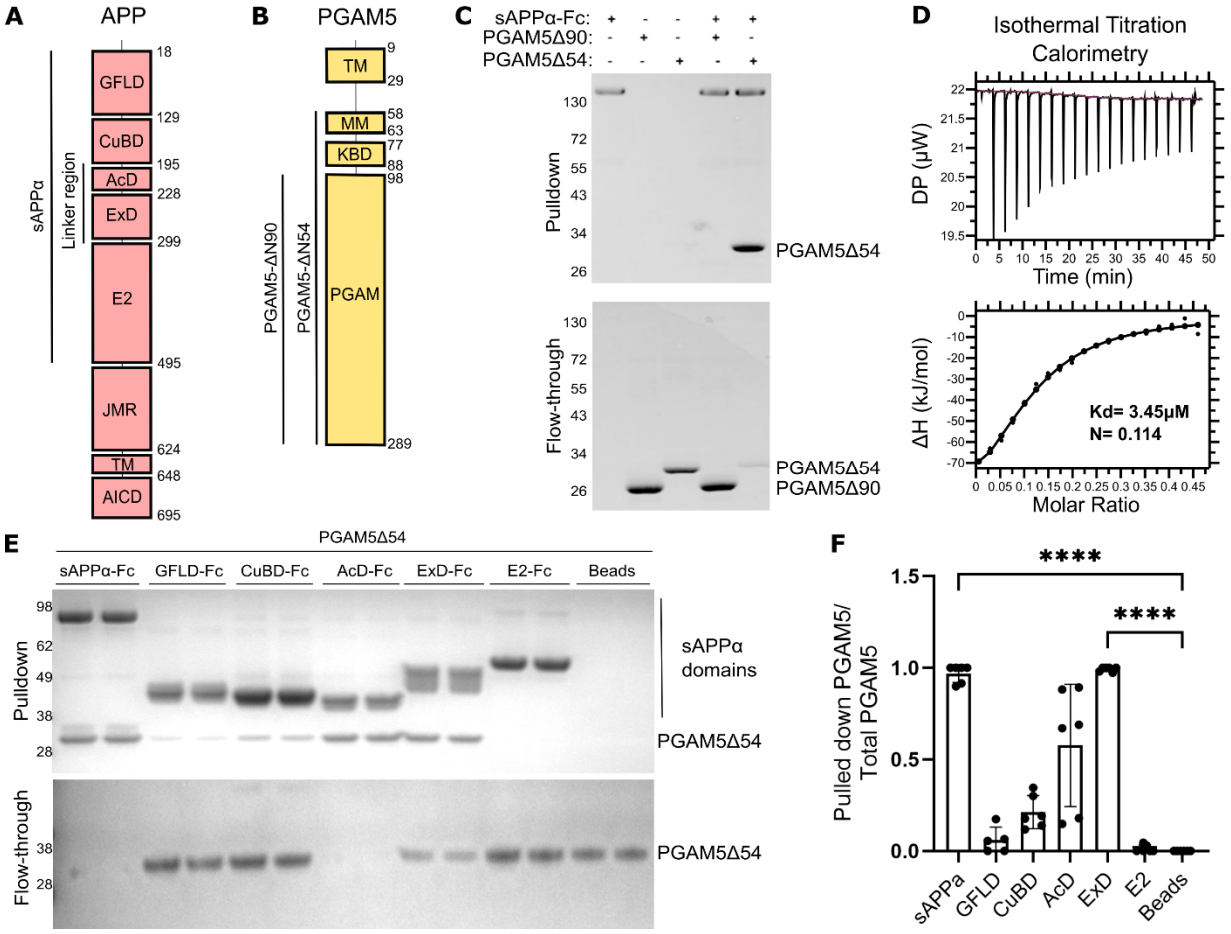
A
APP
sAPPα
Linker region
GFLD
CuBD
AcD
ExD
E2
JMR
TM
AICD
18
129
195
228
299
495
624
648
695
B
PGAM5
TM
MM
KBD
PGAM
PGAM5-ΔN90
PGAM5-ΔN54
9
29
58
63
77
88
98
289
C
sAPPα-Fc:
PGAM5Δ90:
PGAM5Δ54:
Pulldown
Flow-through
PGAM5Δ54
PGAM5Δ54
PGAM5Δ90
D
Isothermal Titration Calorimetry
DP (μW)
Time (min)
ΔH (kJ/mol)
Molar Ratio
Kd= 3.45μM
N= 0.114
E
PGAM5Δ54
sAPPα-Fc
GFLD-Fc
CuBD-Fc
AcD-Fc
ExD-Fc
E2-Fc
Beads
Pulldown
Flow-through
sAPPα domains
PGAM5Δ54
PGAM5Δ54
F
Pulled down PGAM5/ Total PGAM5
****
****
sAPPa
GFLD
CuBD
AcD
ExD
E2
Beads

Figure 3

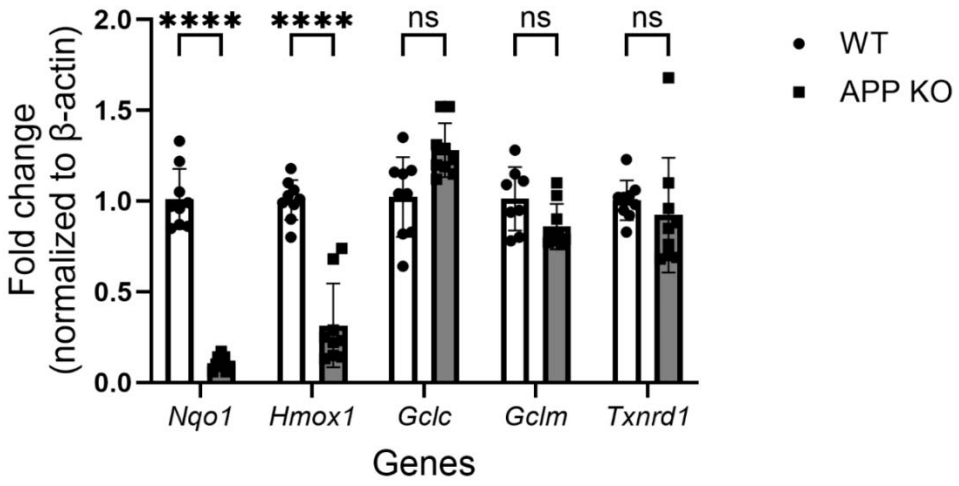
****
****
ns
ns
ns
2.0
1.5
1.0
0.5
0.0
Fold change
(normalized to β-actin)
Nqo1
Hmox1
Gclc
Gclm
Txnrd1
Genes
WT
APP KO

Figure 4

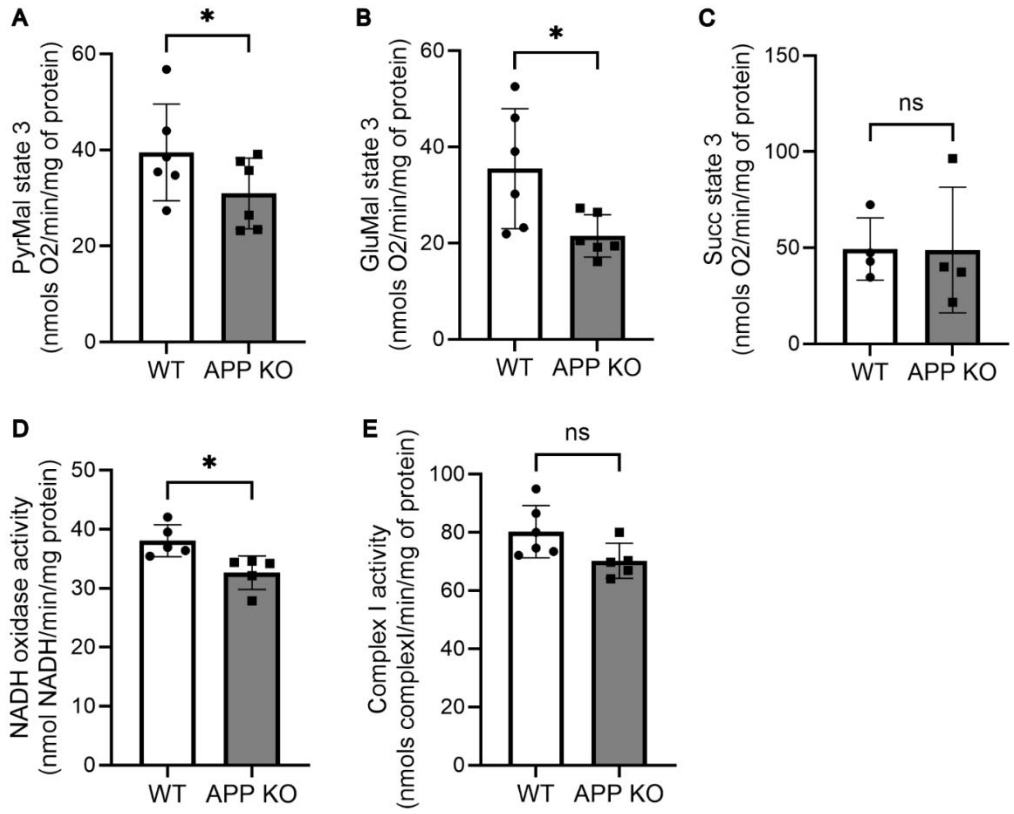
A
PyrMal state 3
(nmols O2/min/mg of protein)
60
40
20
0
*
WT
APP KO
B
GluMal state 3
(nmols O2/min/mg of protein)
60
40
20
0
*
WT
APP KO
C
Succ state 3
(nmols O2/min/mg of protein)
150
100
50
0
ns
WT
APP KO
D
NADH oxidase activity
(nmol NADH/min/mg protein)
50
40
30
20
10
0
*
WT
APP KO
E
Complex I activity
(nmols complexI/min/mg of protein)
100
80
60
40
20
0
ns
WT
APP KO

Figure 5

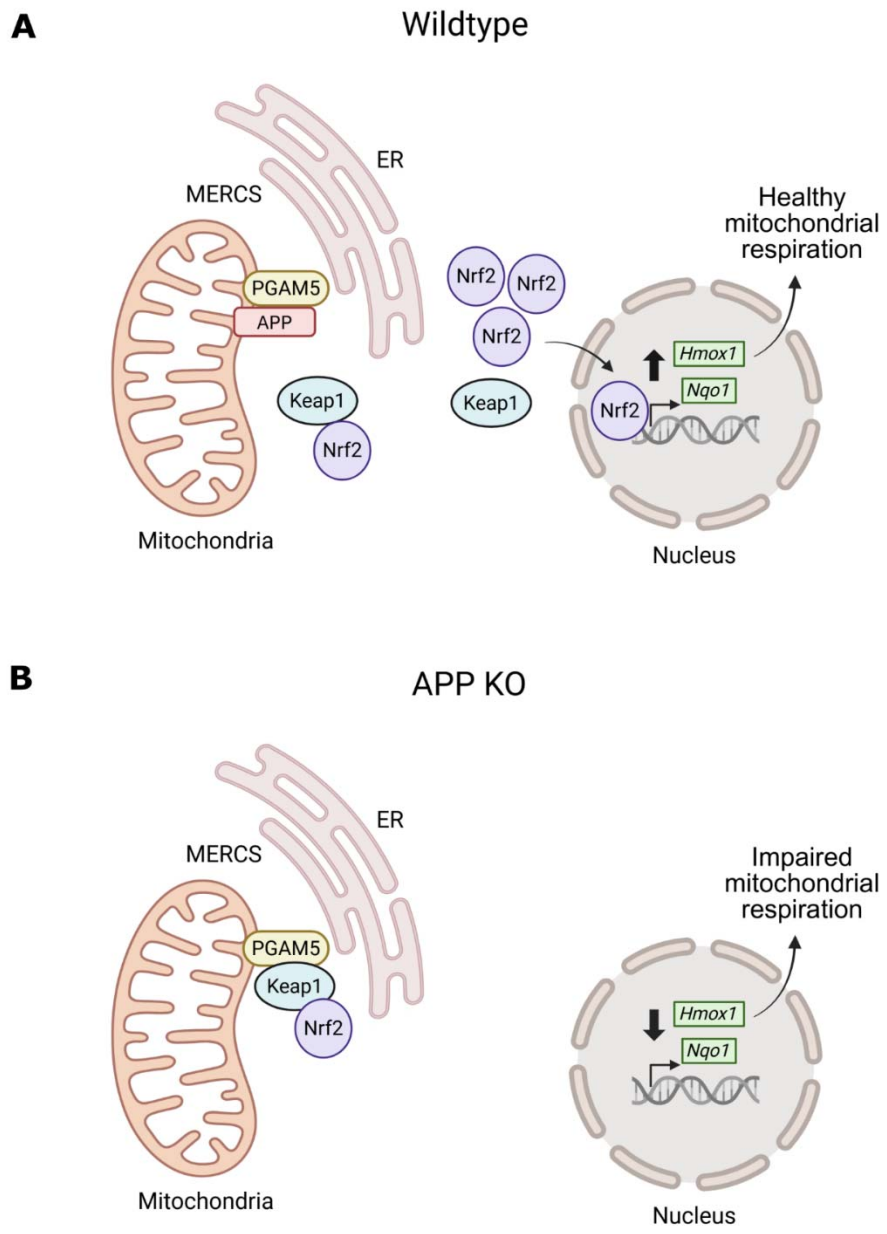
A
Wildtype
ER
MERCS
PGAM5
APP
Keap1
Nrf2
Mitochondria
Nrf2
Nrf2
Nrf2
Keap1
Healthy
mitochondrial
respiration
Hmox1
Nqo1
Nrf2
Nucleus
B
APP KO
ER
MERCS
PGAM5
Keap1
Nrf2
Mitochondria
Impaired
mitochondrial
respiration
Hmox1
Nqo1
Nucleus